Asia-Pacific Journal of Science and Technology: Volume: 29. Issue: 05. Article ID.: APST-29-05-09. Research Article

APST

Asia-Pacific Journal of Science and Technology

https://www.tci-thaijo.org/index.php/APST/index

Published by the Research Department,
Khon Kaen University, Thailand

Quantitative phase analysis of electron beam weldments of copper and stainless steel 304 using XRD and SEM-EDX

Ajith R. Rajendran[1,*], Santhiyagu J. Vijay [2], Dev A. Manoharan[3], Kuzhanthai A. S. Lewise[1], Rimal Isaac[4]

[1]Division of Aerospace Engineering, School of Engineering and Technology, Karunya Institute of Technology & Sciences, Coimbatore, India
[2]Division of Mechanical Engineering, School of Engineering and Technology, Karunya Institute of Technology & Sciences, Coimbatore, India
[3]Director Research, Noorul Islam Centre for Higher Education, Kanyakumari, India
[4]Department of Nanotechnology, Noorul Islam Centre for Higher Education, Kanyakumari, India
[*]Corresponding author: ajithraj@karunya.edu

Received 12 November 2023
Revised 28 December 2023
Accepted 16 February 2024

Abstract

Electron beam welding is performed to join Copper and Stainless steel 304 dissimilar metals for Aerospace applications which demand high-quality defect-free welds. This is a complex process as both the metals possess different material properties. During melting both metals melt and a transition region is formed where both the copper and stainless steel crystals merge together and form weldment. Since both materials possess different properties there are chances for defects or lattice distortion in the interference region. Therefore, the formation of the sigma phase in the weldment is an area of research for material researchers to analyse the crystal structure. In this paper, a quantitative phase analysis is carried out using X-Ray diffraction in the weldment and the crystallographic structure of the weldment grains is found and the behaviour of weldment is analysed towards weld quality.

Keywords: Dissimilar Metal Joints, Electron Beam Welding, Phase Analysis, Microstructural Characterization

1. Introduction

If dissimilar metals could be joined together they could possess various advantages in the aerospace industry since this industry demands less weight and high-strength materials. The existing conventional methods of welding could not make defect-free welds in case of this dissimilar combination since both materials exhibit different physical, chemical and thermal properties [1]. Electron beam welding can be the best source of welding for dissimilar combinations especially for aerospace applications with the optimized input parameters of current and voltage [2,3]. Copper and Stainless Steel dissimilar metal combination has a wide application in the aerospace industry and Electron Beam Welding can produce high precision defect-free dissimilar joints. [4-9]. When a high beam of electron hits the materials they melt and joins together. The volume of metal melts depends on the thermal conductivity and thermal resistivity of the material. The material possesses a low melting point and melts more than the other metal [10]. In this case, copper has the lowest melting point when compared with stainless steel. Therefore the weldment produced will be a Copper alloy with maximum copper contents.

The weldment thus produced as a result of fusion in the interference region should be defect-free and of high strength without porosity. Using X-Ray tomography studies, the welded joints were analysed [11,12]. Detection of Phase Transformation during fusion can be found using X-Ray diffraction analysis [13]. During the fusion of both materials, there are several chances for lattice distortion that may cause defective welds. Using X-Ray diffraction the crystalline structure of the grains and the behaviour of the grain in the weldment can be analysed by determining how the atoms are packed in the crystalline structure [14-16]. Once the packing of the atomic

structure is found we can analyse the properties of the weldment in terms of quality and integrity also. The processing of X-Ray Diffraction (XRD) is done with the help of Inorganic Crystal Structure Database (ICSD) reference data [17,18]. The calculated data are verified numerically and the lattice structure of the grain of the weldment was found out.

From the available literature, it is found that very few researchers have worked on Copper-SS304 dissimilar metal joints and still, there is a lack of evidence to produce high-quality welds. In this investigation Copper and Stainless Steel 304 are joined using Electron Beam Welding and the weldment is subjected to a quantitative analysis using X-ray diffraction. The weldment is analysed towards the quality and integrity by finding the crystalline type and size of grain in the weldment.

2. Materials and methods

2.1 Electron Beam Welding of Copper and Stainless Steel 304

Copper and Stainless steels of size 100 mm x 120 mm x 6 mm each are joined together using Electron Beam welding as shown in Figure 2. The metals are subjected to a pre-weld cleaning and a post-weld cleaning to ensure that the metals are free from impurities that may cause oxidation during welding. The welding is also performed inside a vacuum chamber and therefore no oxidation takes place. Very fine, thin welds are formed with less Heat Affected Zone (HAZ) and with a large depth of penetration. Beam current, Voltage, weld speed and work distance are selected for this study after various trials are 50 mA, 60 kV, 40 mm/s and 260 mm respectively. Fine particles of weldment are taken carefully by filing the weldment and the same has to be used for X-Ray diffraction analysis. Great care was taken during the specimen preparation since the weldment present is of very low thickness and the chances of base metal getting mixed with the powder are higher. During welding, heat conduction happens and the phases are shown in Figure 1.

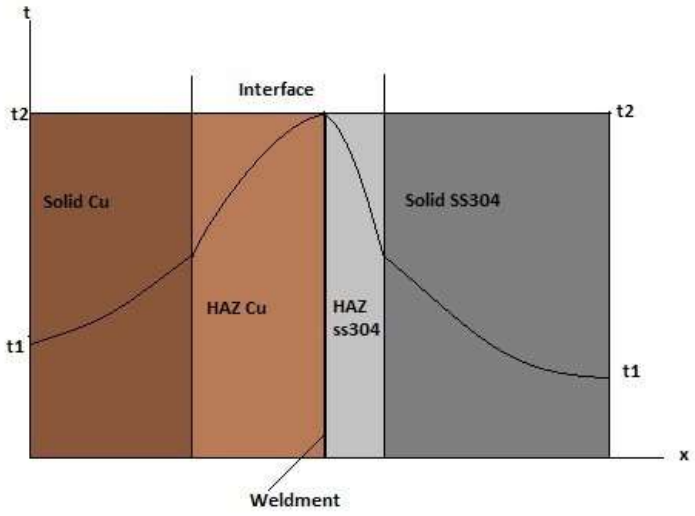

Figure 1 Different Phases during Fusion over time.

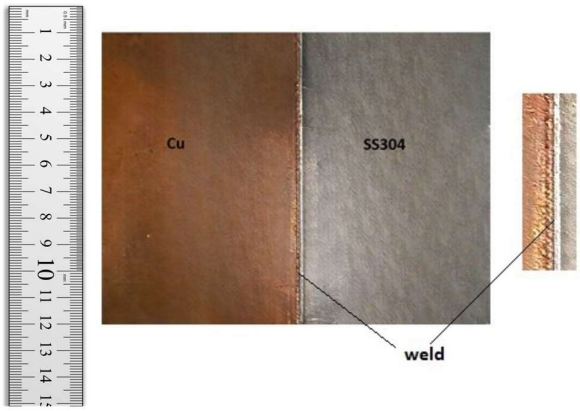

Figure 2 Photographic view of Electron Beam Welded sample of Cu and SS 304.

2.2 X-Ray Diffraction

The prepared specimen is subjected to X-Ray diffraction and the pattern is recorded. The pattern shows the intensity of X-rays scattered by the crystalline material at different angles. 2θ is the scattering angle shown in the X axis and the Y axis shows the respective intensities of scattered X-rays. The peak position is used to identify the crystalline phase of the weldment grains. The strongest and tallest peaks indicate high intensity which can be related to the atoms of the crystal lattice. These strongest and tallest peaks have to be matched with the known crystalline data to correlate the data for the weldment grains.

The lattice parameters can be also found analytically using the Bragg's formula (nλ=2d sinθ) from which the d-spacing values for each peak can be calculated from the equation ($\frac{n\lambda}{2\ sin\theta}$) . For each of the d-spacing values, it is required to calculate the reciprocal of d and then find the smallest whole number ratio among the integers and normalize the values. These normalized reciprocal values correspond to Miller indices (hkl) which represent the crystallographic planes in the crystal lattice. From the Miller indices, lattice parameters a, b and c are calculated which is useful to find the geometry and arrangement of atoms in the crystalline structure. These values can also interpret whether the crystal structure is cubic, tetragonal, monoclinic or triclinic.

2.3 Scanning Electron Microscope-Energy Dispersive X-Ray Analysis (SEM-EDX)

Using X-Ray diffraction analysis, the crystalline structure of the weldment alloy is identified but the other minimal elements present in the weldment can be found using SEM-EDX. The combination of a Scanning Electron Microscope along with the Energy Dispersive X-ray analysis is used to trace the intermittent elements and their presence in the weldment. In order to have a high-integrity weld, the weldment should be free from oxides. This result will show the amount of oxides present in the weldment and the weld can be analysed for its quality and integrity.

3. Results

3.1 X-Ray Diffraction Analysis

The standard JCPDS reference data and the X-ray diffraction pattern obtained for the weldment sample have to be matched. It was discovered that the data closely matches JCPDS cards 70-3039, which displays the data for copper, and 87-0721, which displays the data for iron, and not with any other metals. Figure 3 displays the coupled 2**x** reference peaks from JCPDS cards. Figure 4 displays the X-ray diffraction pattern of the weldment with miller indices. Miller indices for the highest three 2Theta values are shown in Table 1.

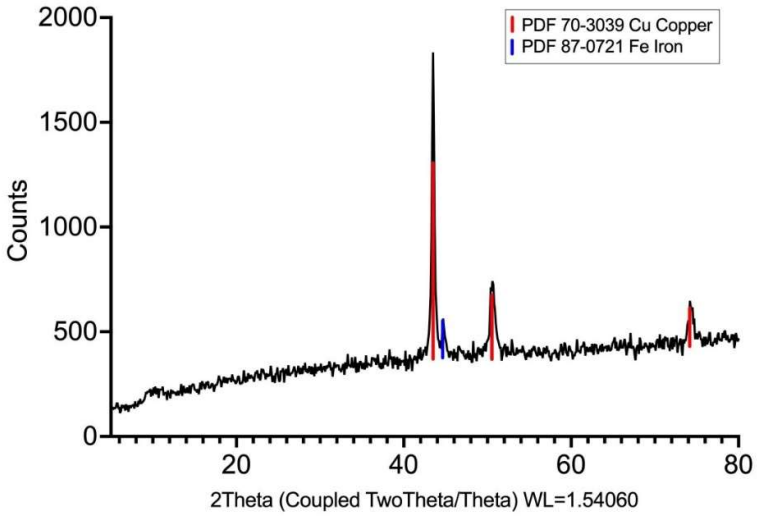

Figure 3 Coupled 2θ reference peaks from JCPDS cards.

Table 1 Miller Indices.

2Theta	d	Miller Indices, h l k
43.4715	2.08006	1 1 1
50.5683	1.80353	2 0 0
74.2443	1.27635	2 2 0

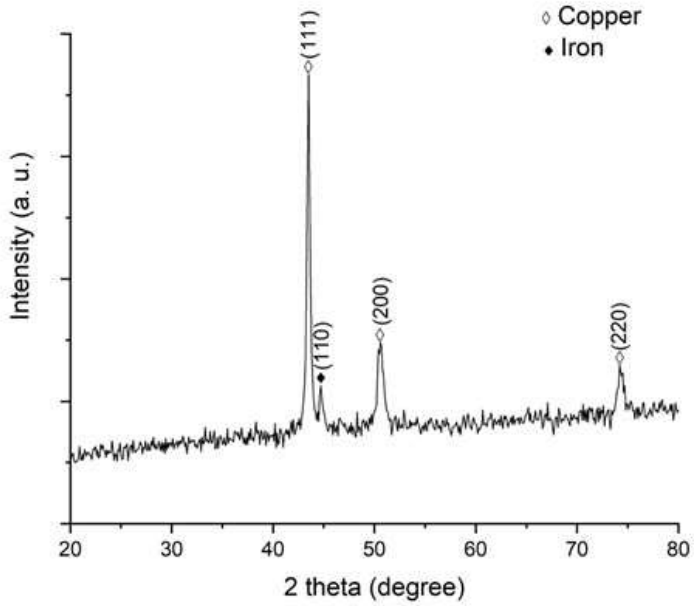

Figure 4 XRD patterns of weld zone with Miller Indices

Miller indices 111 and the associated d value of 2.08006 are selected in order to find the lattice constant which gives $a = 3.60276$ Å. When the reference data is compared to this value of the lattice constant "a" for the weldment, the value is found to be $a = 3.61300$ Å, which is nearly identical to that of the weldment. As a result, both the copper and the stainless steel crystalline structures in the weldment will remain constant, with copper retaining its Face-Centred Cubic (FCC) structure and the iron in the weldment maintaining its FCC structure.

Rietveld refinement was carryout on the XRD data using BRUKER TOPAS v6.0. The results are given in Table 2.

Table 2 Rietveld refinement values of XRD data.

Phase	Crystal Structure	Space Group	Cell Volume (Å3)	Lattice Parameter, a (Å)	Percentage
Copper	Cubic	Fm3m (225)	47.06(19)	3.610(5)	91
Iron	Cubic	Im3m (229)	23.62(17)	2.869(7)	9

The results show that the welded region has 91% copper and 9% iron. This is because the melting point of copper is less than that of stainless steel and copper melts more than stainless steel.

3.2 SEM –EDX

Before the specimen is analyzed using SEM-EDX, it is polished and cut using diamond paste and etching. The surface morphology and microstructure of the weldment are produced by the secondary electrons during electron beam scanning. The surface morphology of the weldment is displayed in Figure 5 at different magnifications. In order to predict the quality of the weld, these images are analyzed to look for the presence of pores, cracks, and fusion lines. The EDX instrument detect and measure the emitted rays. Each element present in the weldment emits X-rays at different characteristic energies. Figure 6 shows the resulting spectrum peaks at different energy levels corresponding to the elements and their quantities within the area chosen for analysis which is also showed in the image. Figure 7 shows the spectrum with various elements present in the weldment and their amount is listed in Table 3.

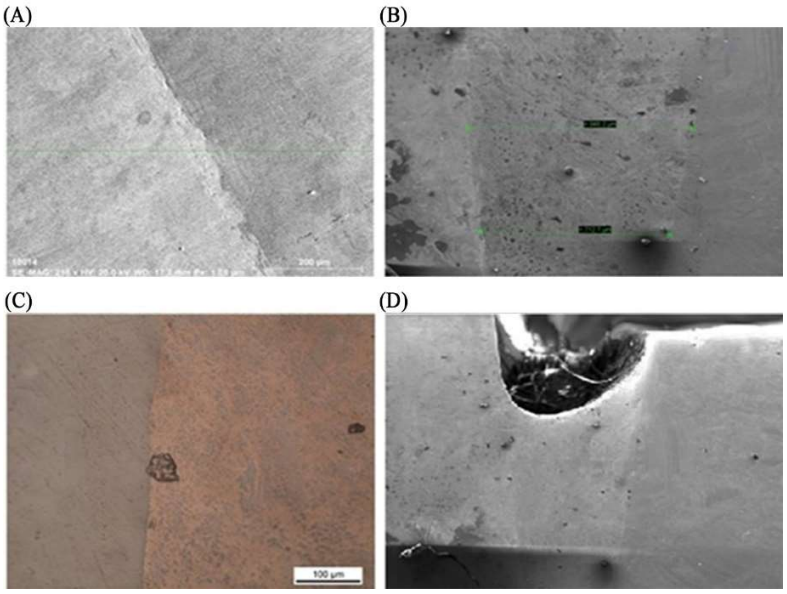

Figure 5 Surface morphology of the weldment (A) 100 µm, (B) 200 µm, (C) 300 µm and (D) 500 µm.

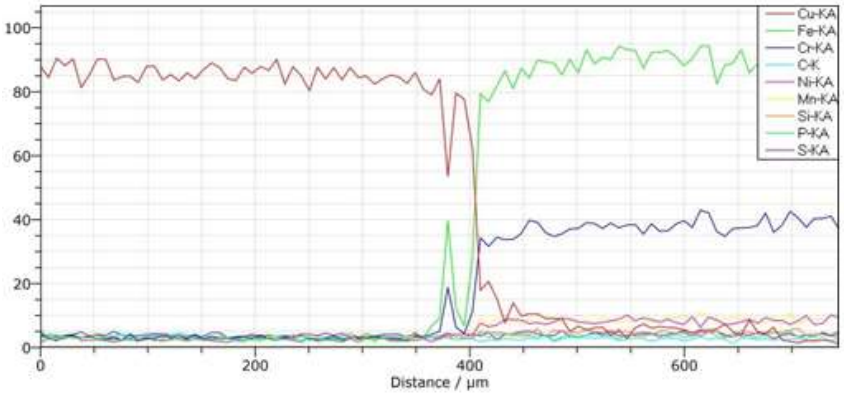

Figure 6 Energy dispersive X-ray Results.

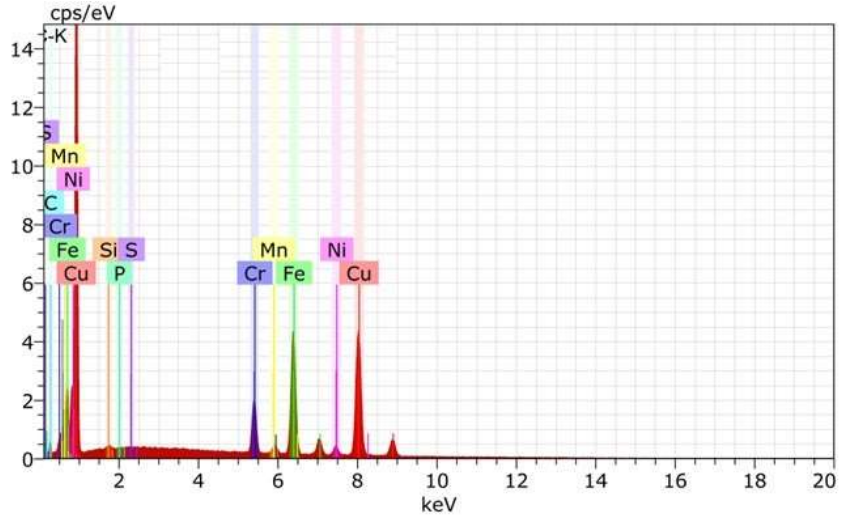

Figure 7 EDX spectrum showing elements in the weldments.

Table 3 Weight percentage of elements present in the weldment.

Elements Present	Weight (%)
Silicon dioxide	2.98
Chromium	11.23
Manganese	0.64
Iron	41.90
Nickel	4.53
Sulphur	0.03
Phosphorous	0.05
Copper	38.64

It is also possible for the EDX detector to determine the elemental composition of the weldment. It is possible to analyze the addition of impurities in the form of oxides and sulphides. The concentration of the elements present can be determined using the specific energy levels of the corresponding elements in the sample provided by this spectra. With 2.98 percent silicon dioxide present, there is very little oxide present in the weldment and no sign of sulphides. This demonstrates the high strength of the formed weldment and the ductility of the weldment's grains due to the absence of oxides. As a result, under stress, the weldment can flex plastically and prevent fracture.

4. Discussion

A dissimilar weld of Copper and Stainless Steel is made using electron beam welding and the weldemnt is subjected to XRD and SEM-EDX analysis to find the weld quality. From the result of XRD analysis, it is evident that the weldment is an alloy primarily composed of iron and copper. The values of Copper with JCPDS card no. 70-3039 and collection code 053247 match up better between the two. This demonstrates that there is more copper than iron in the weldment. The below equation can be used to find the lattice constant value for a cubic lattice structure:

$$\frac{1}{d^2} = \frac{h^2+k^2+l^2}{a^2} \tag{1}$$

Miller indices 111 and the associated d value of 2.08006 are selected in order to find the lattice constant which gives $a = 3.60276$ Å. When the reference data is compared to this value of the lattice constant "a" for the weldment, the value is found to be $a = 3.61300$ Å, which is nearly identical to that of the weldment. [19,20]. As a result, both the copper and the stainless steel crystalline structures in the weldment will remain constant, with copper retaining its FCC structure and the iron in the weldment maintaining its FCC structure.

The SEM images which shows the surface morphology and topology of the weldments at different magnifications does not show any evidence for the presence of major cracks, pores and fusion lines. Figure 7A shows the surface morphology at a 200x magnification, 17.7 mm work distance, and 20kV acceleration. Figure 7B shows the width of the weldment. While analysing Figure 7C we can find few small pores that are present in the weldment. But these pores are very small and does not affect the weld quality. There were no irregularities found in the weldment. Figure 7D shows the topography of the weldment which proves that there were no surface variations in the weldment. The morphology and topology does not show any evidence for the weldment to be more brittle.

The SEM coupled with EDX shows the presence of the elemental composition in the weldment which is recorded in Table 3. It is also possible for the EDX detector to determine the elemental composition of the weldment. It is possible to analyze the addition of impurities in the form of oxides and sulphides. The concentration of the elements present can be determined using the specific energy levels of the corresponding elements in the sample provided by this spectra. With 2.98 percent silicon dioxide present, there is very little oxide present in the weldment and no sign of sulphides. This demonstrates the high strength of the formed weldment and the ductility of the weldment's grains due to the absence of oxides. As a result, under stress, the weldment can flex plastically and prevent fracture.

5. Conclusion

Copper and Stainless Steel 304 are joined using Electron Beam welding. The quality of the weldment towards strength and integrity is analysed using XRD and SEM-EDX analysis. Using XRD it was found that the weldment has more copper content than iron and the crystalline structure of the grains in the weldment is found to be face-centered cubic. SEM-EDX analysis is also performed on the weldment. The morphology of the SEM images shows that the weldment is free from surface cracks and fusion lines. Presence of a few pores are reported but these does not affect the weld quality as they are very small. The element composition is also analyzed using EDX and it was found that the weldment is free from oxides and sulphides which qualifies the weld to be suitable for aerospace applications.

6. Acknowledgments

We express our gratitude to BrahMos Aerospace Thiruvananthapuram Limited for the support provided to execute the dissimilar metal joints of Copper and Stainless Steel 304 using Electron Beam Welding without any charges.

7. References

[1] Poo-arporn Y, Duangnil S, Bamrungkoh D, Klangkaew P, Huasranoi C, Pruekthaisong P, et al. Gas tungsten arc welding of copper to stainless steel for ultra-high vacuum applications. J Mater Process Technol. 2020;277:116490.

[2] Milov AV, Tynchenko VS, Kurashkin SO, Petrenko VE. Approaches review and tools analysis for thermal processes modeling in electron beam welding. J Phys Conf Ser. 2020;1679(5):052008

[3] Rajendran AR, Manoharan DA. A survey on future research about electron beam welding for aerospace applications. China Weld. 2018;7(1):60-64

[4] Vyas HD, Mehta KP, Badheka V, Doshi B. Friction welding of dissimilar joints copper-stainless steel pipe consist of 0.06 wall thickness to pipe diameter ratio. J Manuf Process. 2021;68:1176–1190.

[5] Shanjeevi C, Satish Kumar S, Sathiya P. Multi-objective optimization of friction welding parameters in AISI 304L austenitic stainless steel and copper joints. Proc Inst Mech Eng Part B J Eng Manuf. 2016; 230(3):449–457.

[6] Sahin M. Joining of stainless steel and copper materials with friction welding. Ind Lubr Tribol. 2009; 61(6):319–324.

[7] Li Y, Chen C, Yi R, Ouyang Y. Special brazing and soldering. J Manuf Process. 2020;60:608–635.

[8] Han J, Paidar M, Vignesh RV, Mehta KP, Heidarzadeh A, Ojo OO. Effect of shoulder features during friction spot extrusion welding of 2024-T3 to 6061-T6 aluminium alloys. Arch Civ Mech Eng. 2020;20:1–17.

[9] Kumar D, Kore SD, Nandy A. Finite element modeling of electromagnetic crimping of Cu-SS tube-to-tube joint along with simulation of destructive testing for strength prediction of the joint. J Manuf Sci Eng. 2021;143(4):41004.

[10] Raj, R. A., Anand, M. D., Numerical evaluation of temperature distribution in copper-stainless steel 304 dissimilar metals during electron beam welding. Int J Veh Struct & Syst. 2022;14(3):315-318

[11] Kar J, Dinda SK, Roy GG, Roy SK, Srirangam P. X-ray tomography study on porosity in electron beam welded dissimilar copper--304SS joints. Vacuum. 2018;149:200–206.

[12] Gunavathy K V, Vinoth S, Isaac RSR, Prakash B, Valanarasu S, Trabelsi ABG, et al. Highly improved photo-sensing ability of In2S3 thin films through cerium doping. Opt Mater (Amst). 2023;137:113612.

[13] Rozo Vasquez J, Arian B, Kersting L, Homberg W, Trächtler A, Walther F. Detection of phase transformation during plastic deformation of metastable austenitic steel AISI 304L by Means of X-ray Diffraction Pattern Analysis. Metals. 2023;13(6):1007.

[14] Tashiro K. Crystal Structure Analysis by Wide-Angle X-ray diffraction method. In: Structural science of crystalline polymers: Basic concepts and practices. Springer; 2022. p. 1–285.

[15] Többens DM, Schorr S. The use of anomalous x-ray diffraction as a tool for the analysis of compound semiconductors. Semicond Sci Technol. 2017;32(10):103002.

[16] Otwinowski Z, Minor W. Processing of X-ray diffraction data collected in oscillation mode. In: Methods in enzymology. Elsevier; 1997. p. 307–326.

[17] Cheary R, Ma-Sorrell Y. Quantitative phase analysis by X-ray diffraction of martensite and austenite in strongly oriented orthodontic stainless steel wires. J Mater Sci. 2000;35(5):1105–1113.

[18] Suh I, Ohta H, Waseda Y. High-temperature thermal expansion of six metallic elements measured by dilatation method and X-ray diffraction. J Mater Sci. 1988;23(2):757–760.

[19] Cheary RW, Coelho A. A fundamental parameters approach to X-ray line-profile fitting. J Appl Crystallogr. 1992;25(2):109–121.

[20] Berger H. Study of the Kα emission spectrum of copper. X-Ray Spectrom. 1986;15(4):241–243.